

# Unsteady heat transport in a semi-infinite free end Hooke chain caused by instantaneous heat pulse

Sergei D. Liazhkov

February 2, 2022

## Abstract

We deal with unsteady ballistic heat transport in a semi-infinite Hooke chain with free end caused by instantaneous heat pulse. An analytical description of the evolution of the kinetic temperature is proposed in both discrete and continuum formulations in the frameworks of the lattice dynamics approach. We show analytically a property of thermal wave to reflect from the free end. Continuum description of the transient processes, caused by this reflection, has restrictions. In particular, the kinetic temperature field near the boundary and also evolution of the kinetic temperature at the boundary are inadequately described via the continuum model. Based on the comparison of descriptions of heat propagation in the semi-infinite and infinite Hooke chains, we formulate the principles of symmetry of the discrete and continuum solutions.

## 1 Introduction

Heat transfer at macroscale is known to be diffusive and obeys the Fourier law. Using of the law as constitutive relation, a wide class of problems in continuum mechanics can be solved (see e.g. [1]).

However, recent theory [2, 3] and experiments [4, 5, 6, 7, 9, 8] show that at micro- and nanoscale heat propagation is nondiffusive, e.g. ballistic. In particular, deviation from the Fourier law is shown in nanotubes [4], silicon membranes [6], silicon nanowires [7], graphene [9]. Therefore, development of theory, describing thermal processes at micro- and nano- scale, is required. It is also relevant for development of nanoelectronics (see e.g. [10]).

As a general rule, two approaches are used for description of heat transfer at microscale (or nanoscale), namely the lattice dynamics (LD) approach and investigation of the Boltzmann transport equation (BTE). The second approach implies obtaining a distribution function as solution of BTE, evolution of which is related with motion of quasiparticles (also defined as phonons). Using the kinetic approach, one can solve problems, which are undecidable by the LD (see e.g. [11, 12, 13]) and obtain quantities, continuously changing in space (for instance, the kinetic temperature). Hence there is a question: what circumstances the LD approach to description of non-stationary heat transport problems is needed for? In study [14], a kinetic theory is linked with the LD theory of unsteady heat transport in the infinite one-dimensional harmonic chain. It is shown that solution for the kinetic temperature, obtained by the LD approach, takes into account not only heat transport but the transient process, performing at short times: oscillations of the kinetic temperature caused by equilibration of kinetic and potential energies. In turn, the solution of collisionless BTE is related with heat transport only. In the present paper, we study heat transport in the semi-infinite free end Hooke chain and show that only exact solution by LD approach has information about influences of free end boundary condition on this unsteady process.

Based on the LD, one can distinguish discrete and continuum descriptions of the ballistic heat transport. In the pioneering work of Klein and Prigogine [15] the evolution law of the discrete field (changing in dependence of number of particle) of the kinetic temperature, obtained using exact Schroedinger solution [16] of the dynamics equations for the Hooke chain. In the pioneering work by Krivtsov [18], the PDE for the continuum kinetic temperature (changing in dependence of continuous spatial coordinate) is derived. It follows from this equation that heat transport in harmonic crystals does not obey the Fourier law [19]. In the paper [17], the discrete and continuum kinetic temperature fields are under consideration. It is shown that evolution over time of the temperature fields caused by arbitrary initial perturbation (except point) leads to coincidence of these. However, aforesaid results are only about one-dimensional *infinite* chains.

The question of influences of boundaries, interfaces and inclusions on heat transport remains open. Answer to this is necessary for development of theoretical models of the experiments, related, in particular, with reflection of phonons [20, 21]. This issue is partially addressed in the paper, dedicated to unsteady heat transport in the semi-infinite free end Hooke chain. We expect that obtained in this paper results may serve for generalization to the complex structure lattices.

The paper is organized as follows. In Sect.2, we formulate the problem and derive exact expression for particle velocities by the eigenfunction expansion method. In Sect.3, the formula for velocities is applied to derive the expression for the kinetic temperature. In Sect.4, we perform the continualization for the kinetic temperature to determine this in the continuum limit. In Sect.5 the fundamental solution for the kinetic temperature in continuum limit is found. In Sect.6, the discrete and continuum kinetic temperature fields are in comparison. Examples of the rectangular (Sect.6.2) and step (Sect.6.3) are considered. In Sect.7, we estimate asymptotic behavior of the continuum and discrete kinetic temperature at the boundary. In Sect.8, we compare theory of ballistic heat transport in the semi-infinite Hooke chain with infinite Hooke chain. In Sect.9, the results of the paper are discussed. The principles of symmetry of continuum and discrete solutions for the kinetic temperature are formulated based on results, obtained in Sect.5 and Sect.8 respectively.

## 2 Statement of the problem and exact expression for particle velocities

We consider the Hooke chain with two free ends, which consists of  $N$  particles<sup>1</sup>, interacting with the nearest neighbors. This dynamical system is governed by the dynamics equations

$$\begin{aligned} \dot{u}_n &= v_n, \\ \dot{v}_n &= \omega_e^2(u_{n+1} - 2u_n + u_{n-1}), \quad \omega_e = \sqrt{\frac{c}{m}}, \quad n = 1, \dots, N-2, \\ \dot{v}_0 &= \omega_e^2(u_1 - u_0), \\ \dot{v}_{N-1} &= \omega_e^2(u_{N-2} - u_{N-1}), \end{aligned} \tag{1}$$

where  $u_n$  and  $v_n$  are displacement and velocity for particle  $n$  respectively;  $c$  is the bond stiffness;  $m$  is the mass of a particle. The initial conditions for all particles are as follows:

$$u_n = 0, \quad v_n = v_n^0, \tag{2}$$

where  $v_n^0$  is the initial velocity field.

---

<sup>1</sup>Number of particles  $N$  is constant in time.

Exact solution of the Eq.(1–2) for particle velocities is obtained by the eigenfunction expansion method (see Appendix A):

$$v_n = \frac{2}{N} \sum_{j,k=0}^{N-1} v_j^0 \cos \frac{(2j+1)\pi k}{N} \cos \frac{(2n+1)\pi k}{N} \cos(\omega_k t), \quad \omega_k = 2\omega_e \sin \frac{\pi k}{N}, \quad (3)$$

where  $\omega_k$  is the  $k$ -th eigenfrequency of the chain.

Thus, we have the formula for velocity for each particle in the *finite* chain with two free ends. In the next section, the formula (3) is used to obtain the kinetic temperature.

### 3 Exact expression for the kinetic temperature

We consider an infinite set of realizations, which differ only by the initial conditions (2). For the one-dimensional chain, we can characterize the thermal state via one parameter, which is referred to as the kinetic temperature:

$$m \langle v_n^2 \rangle = k_B T_n, \quad (4)$$

where  $\langle \dots \rangle$  stands for the mathematical expectation sign. Substitution of the formula (3) to the definition of the kinetic temperature (4) yields

$$\frac{k_B}{m} T_n = \frac{4}{N^2} \sum_{i,j,k_1,k_2=0}^{N-1} \langle v_i^0 v_j^0 \rangle \cos \frac{(2i+1)\pi k_1}{N} \cos \frac{(2j+1)\pi k_2}{N} \cos \frac{(2n+1)\pi k_1}{N} \cos \frac{(2n+1)\pi k_2}{N} \cos(\omega_{k_1} t) \cos(\omega_{k_2} t). \quad (5)$$

From (4), the relation of initial velocity for particle  $v_n^0$  and its initial kinetic temperature  $T_n^0$  is

$$v_n^0 = \rho_n \sqrt{\frac{k_B T_n^0}{m}}, \quad \langle \rho_n \rangle = 0, \quad \langle \rho_j \rho_n \rangle = \delta_{jn}, \quad (6)$$

where  $k_B$  is the Boltzmann constant;  $\delta_{jn}$  is the Kronecker delta;  $T_n^0$  is the initial kinetic temperature of particle  $n$  (see definition (4));  $\rho_n$  are uncorrelated random numbers with zero mean and unit variance. Thus, the initial conditions (2) imply an existence of a some initial temperature field in the chain and zero initial heat fluxes can be considered as a model of heating of the crystal by ultrashort laser pulse. Uncorrelation of the initial velocities results in

$$T_n = \frac{4}{N^2} \sum_{j=0}^{N-1} T_j^0 \left( \sum_{k=0}^{N-1} \cos \frac{(2j+1)\pi k}{N} \cos \frac{(2n+1)\pi k}{N} \cos(\omega_k t) \right)^2. \quad (7)$$

The formula (7) is the exact expression for the discrete kinetic temperature for the chain with two free ends.

We assume that the right end of the chain is located infinitely far away from the domain, wherein the thermal pulse could be concentrated. This assumption allows us to proceed to the thermodynamic limit ( $N \rightarrow \infty$ ) and refer the chain as the *semi-infinite free end chain*. We introduce the new variable  $\theta = 2\pi k/N$  and replace the sum with respect to the number  $k$  to the corresponding integral over the interval, symmetric to zero:

$$T_n = \frac{1}{\pi^2} \sum_{j=0}^{\infty} T_j^0 \left( \int_{-\pi}^{\pi} \cos \frac{(2j+1)\theta}{2} \cos \frac{(2n+1)\theta}{2} \cos(\omega(\theta)t) d\theta \right)^2, \quad (8)$$

where  $\omega(\theta) = 2\omega_e \sin \frac{\theta}{2}$  is the dispersion relation.

The formula (8) is an exact solution for the discrete kinetic temperature of the semi-infinite chain with free end. If we decompose the product of cosines in (8) to sum of complex exponents, we obtain the representation of the kinetic temperature as superposition of waves with wavenumber  $\theta$ . We further refer (8) to as a *discrete solution*.

The expression (8) is further employed to obtain the kinetic temperature in the continuum limit.

## 4 Kinetic temperature in the continuum limit

In the section, we derive the kinetic temperature in continuum limit, namely is a function of continuum generalized coordinate. We show, in particular, that the final expression is represented as the superposition of wave packets.

We use an approach, proposed in study [14]. First of all, we separate the formula (8) into two terms, corresponding to the two physical processes:

$$\begin{aligned}
 T_n &= T_n^F + T_n^S, \\
 T_n^F &= \sum_{j=0}^{\infty} T_j^0 F_{nj}, \quad T_n^S = \sum_{j=0}^{\infty} T_j^0 S_{nj}, \\
 F_{nj} &= \frac{1}{2\pi^2} \iint_{-\pi}^{\pi} \cos \frac{(2j+1)\theta_1}{2} \cos \frac{(2j+1)\theta_2}{2} \cos \frac{(2n+1)\theta_1}{2} \cos \frac{(2n+1)\theta_2}{2} \cos ((\omega(\theta_1) + \omega(\theta_2))t) d\theta_1 d\theta_2, \\
 S_{nj} &= \frac{1}{2\pi^2} \iint_{-\pi}^{\pi} \cos \frac{(2j+1)\theta_1}{2} \cos \frac{(2j+1)\theta_2}{2} \cos \frac{(2n+1)\theta_1}{2} \cos \frac{(2n+1)\theta_2}{2} \cos ((\omega(\theta_1) - \omega(\theta_2))t) d\theta_1 d\theta_2.
 \end{aligned} \tag{9}$$

We further show that the first term corresponds to high-frequency oscillations of the kinetic temperature, caused by equilibration of the kinetic and potential energies [24]. This is a fast process, occurring in time of order of several atomic periods. The second term corresponds to the slow process caused by ballistic heat transport. Using the following assumption, we perform a continualization for the «slow» and «fast» terms of the kinetic temperature,  $T^S$ .

### 4.1 Slow term

We introduce a mesoscale, which is larger than the distance between particles,  $a$ , but smaller than a some macroscale <sup>2</sup>,  $\mathcal{A}$  and divide the chain into the equal intervals, indexed by  $s$ . Each interval  $s$  has the length  $2a\Delta N$ ,  $\Delta N \gg 1$ ,  $a\Delta N \ll \mathcal{A}$  and is limited by the boundary-particles,  $j_s$ . We assume that the initial temperature profile enclosed in the intervals  $s$  slowly changes in time.

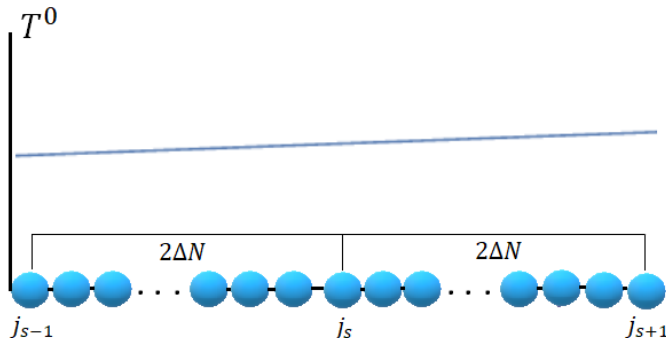


Figure 1: Initial temperature profile.

<sup>2</sup>A macroscale can be interpreted as a scale of the order of the length of chain.

Therefore, the length of the mesoscale is  $2a\Delta N$ . Then, the expression for  $T_n^S$  in the formula (9) can be rewritten as

$$\begin{aligned} T_n^S &= \sum_{s=0}^{\infty} \sum_{j=j_s-\Delta N+1}^{j_s+\Delta N} T_j^0 S_{nj} \approx \sum_{s=0}^{\infty} T_{j_s}^0 \sum_{j=j_s-\Delta N+1}^{j_s+\Delta N} S_{nj} \\ &= 2a\Delta N \sum_{s=0}^{\infty} T_{j_s}^0 g_{n,j_s}^S(\Delta N), \quad g_{n,j_s}^S(\Delta N) = \frac{1}{2a\Delta N} \sum_{j=j_s-\Delta N+1}^{j_s+\Delta N} S_{nj}, \end{aligned} \quad (10)$$

where  $g_{n,j_s}^S(\Delta N)$  determines contribution of the point  $j_s$  to the temperature at point  $n$ . It can also be interpreted as a discrete fundamental solution, obtained by averaging of the  $T_n^S$  over the mesoscale. The following formula for  $g_{n,j_s}^S(\Delta N)$  is calculated up to the order  $O\left(\frac{1}{\Delta N}\right)$  (see Appendix B) and is represented below:

$$\begin{aligned} g_{n,j_s}^S(\Delta N) &\approx \frac{1}{16\pi^2 a} \iint_{-\pi}^{\pi} \left[ \cos(\Delta\theta\omega'(\theta_1)t) \cos((n+j_s)\Delta\theta) \text{sinc}(\Delta N\Delta\theta) \right] d\theta_1 d\theta_2 + \\ &\frac{1}{16\pi^2 a} \iint_{-\pi}^{\pi} \left[ \cos(\Delta\theta\omega'(\theta_1)t) \cos((n-j_s)\Delta\theta) \text{sinc}(\Delta N\Delta\theta) \right] d\theta_1 d\theta_2 + \\ &\frac{1}{16\pi^2 a} \iint_{-\pi}^{\pi} \left[ \cos(\Delta\theta\omega'(\theta_1)t) \cos(\theta_1(2n+1) - (n+j_s)\Delta\theta) \text{sinc}(\Delta N\Delta\theta) \right] d\theta_1 d\theta_2 + \\ &\frac{1}{16\pi^2 a} \iint_{-\pi}^{\pi} \left[ \cos(\Delta\theta\omega'(\theta_1)t) \cos(\theta_1(2n+1) - (n-j_s)\Delta\theta) \text{sinc}(\Delta N\Delta\theta) \right] d\theta_1 d\theta_2, \end{aligned} \quad (11)$$

where  $\Delta\theta = \theta_1 - \theta_2$ ,  $(\cdot)' = \frac{d}{d\theta_1}$ ,  $\text{sinc}(x) = \frac{\sin x}{x}$ . We change the variables  $\theta = \theta_1$ ,  $q = \Delta\theta$  and rewrite the formula (11), using trigonometric identities and symmetry of the integrands with respect to zero:

$$\begin{aligned} g_{n,j_s}^S(\Delta N) &= \frac{1}{8\pi} \int_0^{\pi} \left[ \psi_1(n+j_s+\omega'(\theta)t) + \psi_1(n+j_s-\omega'(\theta)t) \right] d\theta \\ &+ \frac{1}{8\pi} \int_0^{\pi} \left[ \psi_1(n-j_s+\omega'(\theta)t) + \psi_1(n-j_s-\omega'(\theta)t) \right] d\theta \\ &+ \frac{1}{8\pi} \int_0^{\pi} \cos(\theta(2n+1)) \left[ \psi_1(n+j_s+\omega'(\theta)t) + \psi_1(n+j_s-\omega'(\theta)t) \right] d\theta \\ &+ \frac{1}{8\pi} \int_0^{\pi} \cos(\theta(2n+1)) \left[ \psi_1(n-j_s+\omega'(\theta)t) + \psi_1(n-j_s-\omega'(\theta)t) \right] d\theta \\ &+ \frac{1}{8\pi} \int_0^{\pi} \sin(\theta(2n+1)) \left[ \psi_2(n+j_s+\omega'(\theta)t) + \psi_2(n+j_s-\omega'(\theta)t) \right] d\theta \\ &+ \frac{1}{8\pi} \int_0^{\pi} \sin(\theta(2n+1)) \left[ \psi_2(n-j_s+\omega'(\theta)t) + \psi_2(n-j_s-\omega'(\theta)t) \right] d\theta, \\ \psi_1(\Xi) &= \frac{1}{2\pi a} \int_{\theta-\pi}^{\theta+\pi} \cos(\Xi q) \text{sinc}(q\Delta N) dq, \\ \psi_2(\Xi) &= \frac{1}{2\pi a} \int_{\theta-\pi}^{\theta+\pi} \sin(\Xi q) \text{sinc}(q\Delta N) dq, \end{aligned} \quad (12)$$

where  $\psi_1$  and  $\psi_2$  are referred to as wave packets propagating with group velocity  $v_g = a\omega'$ . Averaging of the function  $g_{n,j_s}^S$  over mesoscale leads to a sum of the integrals of these wave

packets. In the limit case ( $\Delta N \gg 1$ ) the wave packet  $\psi_2$  is negligible and the expression for  $\psi_1$  has the following approximate form (see Appendix C):

$$\psi_1(\Xi) \approx \frac{1}{2a\Delta N} H\left(1 - \frac{|\Xi|}{\Delta N}\right), \quad (13)$$

where  $H(x)$  is the Heaviside function. Using the limit case for  $\Delta N$ , we obtain the final form of the discrete fundamental solution:

$$\begin{aligned} g_{n,j_s}^S(\Delta N) &\approx \frac{1}{4\pi} \int_0^\pi \left[ \psi(n - j_s + \omega'(\theta)t, \Delta N) + \psi(n - j_s - \omega'(\theta)t, \Delta N) \right] d\theta \\ &+ \frac{1}{4\pi} \int_0^\pi \left[ \psi(n + j_s + \omega'(\theta)t, \Delta N) + \psi(n + j_s - \omega'(\theta)t, \Delta N) \right] d\theta, \\ \psi(\Xi, \Delta N) &= \frac{1}{2a\Delta N} \cos^2\left(\frac{\theta(2n+1)}{2}\right) H\left(1 - \frac{|\Xi|}{\Delta N}\right). \end{aligned} \quad (14)$$

We introduce continuous functions  $T^S(x)$ ,  $T^0(x)$ ,  $g_c^S(x, y)$  such that

$$\begin{aligned} T^0(an) &= T_n^0, \quad g_c^S(x, y) = \lim_{\frac{a\Delta N}{\mathcal{A}} \rightarrow 0} g_{n,j_s}^S(\Delta N), \\ T^S(x) &= \lim_{\frac{a\Delta N}{\mathcal{A}} \rightarrow 0} T_n^S = \int_0^\infty T^0(y) g_c^S(x, y) dy. \end{aligned} \quad (15)$$

In the limit case  $a\Delta N/\mathcal{A} \rightarrow 0$ , the function  $\psi$  can be replaced by the Dirac delta function. Using formulas (14), (15), we obtain the fundamental solution for the slow term of the kinetic temperature:

$$\begin{aligned} g_c^S(x, y) &= \frac{1}{4\pi} \int_0^\pi \left[ \delta(x - y + v_g(\theta)t) + \delta(x - y - v_g(\theta)t) \right] d\theta \\ &+ \frac{1}{4\pi} \int_0^\pi \left[ \delta(x + y + v_g(\theta)t) + \delta(x + y - v_g(\theta)t) \right] d\theta, \quad v_g(\theta) = v_s \cos \frac{\theta}{2}, \end{aligned} \quad (16)$$

where  $v_g(\theta)$  is the group velocity;  $v_s = a\omega_e$  is the sound velocity.

Therefore, the continuum fundamental solution  $g_c^S$  is represented as superposition of *independent* localized wave packets, propagating with group velocities, so heat propagates *ballistically*. The slow term  $T^S$  is further obtained as the integral convolution of this fundamental solution with field of the initial temperature. Substituting of the formula (16) to (15) yields

$$\begin{aligned} T^S &= \frac{1}{4\pi} \int_0^\pi \left[ T^0(x + v_g(\theta)t)H(x + v_g(\theta)t) + T^0(x - v_g(\theta)t)H(x - v_g(\theta)t) \right] d\theta \\ &+ \frac{1}{4\pi} \int_0^\pi \left[ T^0(-x - v_g(\theta)t)H(-x - v_g(\theta)t) + T^0(-x + v_g(\theta)t)H(-x + v_g(\theta)t) \right] d\theta, \end{aligned} \quad (17)$$

Since  $x \geq 0$  and  $v_g(\theta) \geq 0$  at  $\theta \in [0; \pi]$ , then the formula (17) is simplified:

$$T^S = \frac{1}{2\pi} \int_0^\pi T^0(|x + v_s t \cos \theta|) d\theta. \quad (18)$$

The expression (18) shows that the solution of heat transfer problem in semi-infinite chain is represented as a superposition of wave packets.

## 4.2 Fast term

In this subsection, we derive the «fast» term of the kinetic temperature  $T^F(x)$ , corresponding to equilibration of the kinetic and potential energies. Using the assumption (10) with  $a\Delta N \ll \mathcal{A}$  and  $\Delta N \gg 1$ , we introduce continuous functions  $T^F(x)$ ,  $g_c^F(x, y)$  such that

$$\begin{aligned} T^F(x) &= \lim_{\frac{a\Delta N}{\mathcal{A}} \rightarrow 0} T_n^F = \int_0^\infty T^0(y) g_c^F(x, y) dy, \\ g_c^F(x, y) &= \lim_{\frac{a\Delta N}{\mathcal{A}} \rightarrow 0} g_{n, j_s}^F(\Delta N), \quad g_{n, j_s}^F(\Delta N) = \frac{1}{2a\Delta N} \sum_{j=j_s-\Delta N+1}^{j_s+\Delta N} F_{nj}. \end{aligned} \quad (19)$$

Since the main contribution to the terms  $T^F$  comes from points  $\theta_1 \approx \theta_2$ , as it was shown in Sect.4.2, then  $\omega(\theta_1) + \omega(\theta_2) \approx 2\omega(\theta_1)$ . According to Sect. 4.1, the fundamental solution,  $g_c^F$ , can be written as

$$g_c^F(x, y) = \frac{\delta(x-y) + \delta(x+y)}{2\pi} \int_0^\pi \cos(2\omega(\theta)t) d\theta = \frac{\delta(x-y) + \delta(x+y)}{2} J_0(4\omega_\epsilon t), \quad (20)$$

where  $J$  is the Bessel function of the first kind. Then, the formula for  $T^F$  has the form

$$T^F = \frac{T^0(x)H(x) + T^0(-x)H(-x)}{2} J_0(4\omega_\epsilon t) = \frac{T^0(x)}{2} J_0(4\omega_\epsilon t). \quad (21)$$

Therefore, the expression for the fast term of the kinetic temperature,  $T^F$  coincides with the same formula for the infinite chain [24].

Finally, the expression for the continuum kinetic temperature in the semi-infinite chain is

$$T(x, t) = \frac{T^0(x)}{2} J_0(4\omega_\epsilon t) + \frac{1}{2\pi} \int_0^\pi T^0(|x + v_s t \cos \theta|) d\theta. \quad (22)$$

Thus, the final expression for the kinetic temperature in the continuum limit is the sum of the contribution of fast processes caused by equilibration of kinetic and potential energies ( $T^F$ ) and contribution of slow processes caused by ballistic heat transport ( $T^S$ ). We further refer the formula (22) to as a *continuum solution*.

*Remark* In the [14], the heat transport in the infinite Hooke chain is investigated in the frameworks both of the lattice dynamics approach and of the Boltzmann kinetic theory. By the second approach, solution for the continuum kinetic temperature is derived using the distribution function as solution of the collisionless Boltzmann transport equation. The result coincides with predictions from the lattice dynamics approach. As for the semi-infinite free end Hooke chain, the kinetic temperature can be obtained in the same way, if the solution of the collisionless Boltzmann transport equation with even parity condition at the boundary ( $x = 0$ ) is known. The result must coincide with (18).

## 5 Point heat perturbation. Principle of continuum solution symmetry

We consider the point instantaneous thermal perturbation in the point, located at a some distance from the boundary <sup>3</sup> namely  $ha$ ,  $h \in \mathbb{N} \cup \{0\}$ . Determine the initial temperature, corresponding to the considered case:

$$T^0(x) = A\delta(x - ha), \quad (23)$$

---

<sup>3</sup>Here and further, the left free end is referred to as boundary.

where  $A$  is a constant with dimension  $K \cdot m$ . Since thermal equilibration occurs instant, we neglect the fast term,  $T^F$ . Therefore,

$$T = \frac{A}{2\pi} \int_0^\pi \delta(|x + v_s \cos \theta t| - ha) d\theta. \quad (24)$$

Calculation of integrals (24) is carried out using the following formula [25]:

$$\int_{\mathcal{D}} \delta(f(\Xi)) d\Xi = \sum_i \frac{1}{|f'(\Xi_i)|}, \quad f(\Xi) = 0, \quad (25)$$

where  $\Xi_i$  are zeros of function  $f$ , lying inside the domain  $\mathcal{D}$ . Therefore, we have the following formula for the continuum kinetic temperature

$$T = \frac{A}{2\pi} \left( \frac{H(v_s t - |x - ha|)}{\sqrt{v_s^2 t^2 - (x - ha)^2}} + \frac{H(v_s t - |x + ha|)}{\sqrt{v_s^2 t^2 - (x + ha)^2}} \right). \quad (26)$$

We have obtained the continuum temperature in the semi-infinite chain in the case of a heat pulse. However, if we consider the infinite chain with thermal sources located at the points  $ha$  and  $-ha$ , the obtained continuum solution is the same [22].

Thus, the continuum kinetic temperature in the semi-infinite Hooke chain with free end and some source *coincides* with the continuum kinetic temperature in the infinite Hooke chain with the same and mirrored sources. The aforesaid rule will be further referred to as a *principle of continuum solution symmetry*.

The formula (26) shows (respectively to the infinite chain) behavior of thermal waves, travelling to the both directions from the points  $x = ha$  and  $x = -ha$ . The wave, emanated from the point  $x = ha$  and travelling to the point  $x = 0$ , collides with the wave, travelling from the point  $x = -ha$  at the moment  $t = ha/v_s$ . As for semi-infinite chain, the emanated wave from the point  $x = ha$ , travelling to the left end ( $x = 0$ ), *instantly* reflects at moment  $t = ha/v_s$  from the left end and travels backwards.

We consider point heat perturbation, located at some point from the boundary ( $h = 10$ ). Behavior of thermal waves, propagation of which obeys the formula (26) is represented in figure 2.

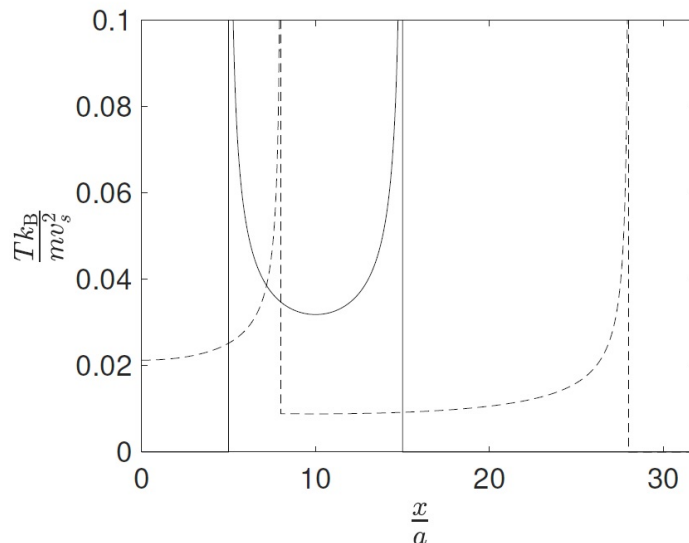


Figure 2: Thermal waves.  $\omega_e t = 5$  (solid line),  $\omega_e t = 18$  (dashed line).

Figure 2 shows travelling to both directions waves before reflection ( $\omega_e t < 10$ ) and backwards after the reflection ( $\omega_e t > 10$ ). Specifically, it is shown that, the temperature profile is not symmetric with respect to the heat source after the reflection.

Thus, we have analytically described a property of the ballistically propagating thermal waves to reflect from boundaries.

## 6 Examples

In this section, evolution of the kinetic temperature fields in the cases of rectangular and step thermal perturbations are under investigation. We compare discrete and continuum temperature fields and show that continuum descriptions of heat transport have some restrictions.

### 6.1 Simulation details

For further analyzing of derived formulas for the kinetic temperatures, we make these dimensionless. First of all, we introduce the following dimensionless variables  $\tilde{x}$ ,  $\tilde{u}$ ,  $\tilde{v}$ ,  $\tilde{t}$ ,  $\tilde{T}$  such as:

$$\begin{aligned}\tilde{x} &= x/a, & \tilde{u} &= u/a, \\ \tilde{v} &= v/v_s, & \tilde{t} &= \omega_e t, & \tilde{T} &= Tk_B/(mv_s^2).\end{aligned}\tag{27}$$

In the points of particle locations  $\tilde{x} \equiv n$ . We denote further the continuum kinetic temperature as  $\tilde{T}(\tilde{x})$  and the discrete kinetic temperature as  $\tilde{T}_n$ .

We rewrite the dynamics equations (1) as

$$\begin{aligned}\frac{d\tilde{u}_n}{d\tilde{t}} &= v_n, \\ \frac{d\tilde{v}_n}{d\tilde{t}} &= \tilde{u}_{n+1} - 2\tilde{u}_n + \tilde{u}_{n-1}, & n &= 1, 2, \dots, N-2, \\ \frac{d\tilde{v}_{N-1}}{d\tilde{t}} &= \tilde{u}_{N-2} - \tilde{u}_{N-1}, \\ \frac{d\tilde{v}_0}{d\tilde{t}} &= \tilde{u}_1 - \tilde{u}_0,\end{aligned}\tag{28}$$

with initial conditions

$$\tilde{u}_n = 0, \quad \tilde{v}_n = \frac{d\tilde{u}_n}{d\tilde{t}} = \rho_n \sqrt{\tilde{T}_n^0}, \quad \langle \rho_n \rangle = 0, \quad \langle \rho_m \rho_n \rangle = \delta_{mn}.\tag{29}$$

In numerical simulations, the kinetic temperatures are calculated numerically as follows:

$$\tilde{T}_n = \frac{1}{R} \sum_{i=1}^R \tilde{v}_{n,i}^2,\tag{30}$$

where  $R$  is number of realizations, which differs by random initial conditions (29),  $R = 10^5$ . Particle velocity,  $\tilde{v}_{n,i}$ , is obtained for each realization  $i$  via solving of dynamics equations<sup>4</sup> (28) with initial conditions<sup>5</sup> (29) using the fourth-order symplectic Candy and Rozmus integrator [27] with optimizing parameters proposed in [28] and time-step  $\Delta\tilde{t} = 0.01$ .

Analytical discrete and continuum solutions for the kinetic temperature are respectively rewritten as

<sup>4</sup>The chain with  $N = 500$  particles is used. For that,  $\tilde{t}$  is taken to be less than the time of thermal wave propagation to the right end.

<sup>5</sup>Random numbers  $\rho_n$  are uniformly distributed in the segment  $[-\sqrt{3}; \sqrt{3}]$ .

$$\tilde{T}_n = \frac{1}{\pi^2} \sum_{j=0}^{\infty} \tilde{T}_j^0 \left( \int_{-\pi}^{\pi} \cos \frac{(2j+1)\theta}{2} \cos \frac{(2n+1)\theta}{2} \cos \left( 2\tilde{t} \sin \frac{\theta}{2} \right) d\theta \right)^2, \quad (31)$$

$$\tilde{T}(\tilde{x}, \tilde{t}) = \frac{\tilde{T}^0(\tilde{x})}{2} J_0(4\tilde{t}) + \frac{1}{2\pi} \int_0^{\pi} \tilde{T}^0(|\tilde{x} + \tilde{t} \cos \theta|) d\theta. \quad (32)$$

## 6.2 Rectangular initial perturbation

Consider a rectangular heat perturbation, which is defined by following formula:

$$\tilde{T}^0(\tilde{x}) = H(\tilde{x} - \tilde{L}_1) - H(\tilde{x} - (\tilde{L}_1 + \tilde{L}_2)), \quad \tilde{L}_1 > 0, \tilde{L}_2 > 0, \quad (33)$$

where  $\tilde{L}_1 a$  is a distance from the boundary to the perturbation,  $\tilde{L}_2 a$  is a width of perturbation. We take  $\tilde{L}_1 = 25$  and  $\tilde{L}_2 = 50$  and investigate temperature profiles in two cases: before reflection of thermal wave and after reflection. Discrete and continuum kinetic temperatures, corresponding to the case before reflection, are represented in figure 3.

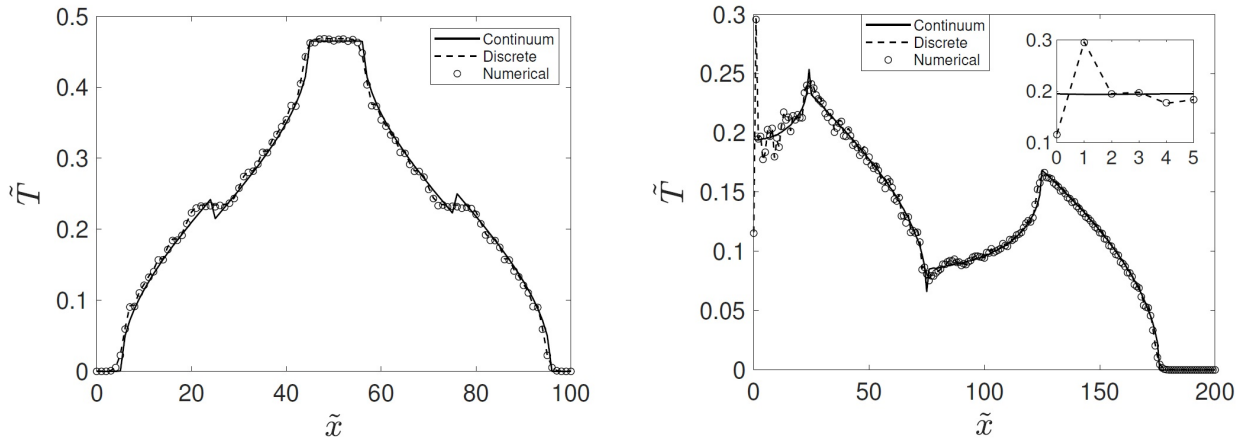


Figure 3: Discrete and continuum solutions for kinetic temperature in the semi-infinite Hooke chain, in the case of rectangular initial perturbation.  $\tilde{t} = 20$  (left) and  $\tilde{t} = 100$  (right).

It is seen in figure 3 (left) that the continuum and discrete solutions practically coincide before thermal wave reaches the boundary, except regions near wavefront and on the boundaries of initial perturbation. Aforesaid mismatches are caused by finiteness of the perturbation length and fast process, which takes place at relatively short times. The mismatches, mentioned above become infinitesimal at  $\tilde{t} = 100$  (see right Fig. 3), when energy of the fast process is much less than energy transferred along the chain. However, the discrete kinetic temperature undergoes a jump near the boundary (see inlet of right Fig. 3). Therefore, after reflection of thermal wave from the boundary, the discrete and continuum solutions *disagree*. In order to investigate this jump in detail, let us consider behavior of the temperatures at the boundary.

The formula for the continuum temperature at the boundary,  $\tilde{T}(0, \tilde{t})$ , has the following form, which can be obtain by substitution of (33) to (32) with  $\tilde{x} = 0$  and subsequent integration from 0 to  $\pi$ :

$$\tilde{T}(0, \tilde{t}) = \frac{1}{\pi} \left( \arccos \left( \frac{\tilde{L}_1}{\tilde{t}} \right) H(\tilde{t} - \tilde{L}_1) - \arccos \left( \frac{\tilde{L}_1 + \tilde{L}_2}{\tilde{t}} \right) H(\tilde{t} - (\tilde{L}_1 + \tilde{L}_2)) \right). \quad (34)$$

From the formula 34, one can conclude that evolution of the kinetic temperature at the boundary, caused by rectangular perturbation in the chain, has three stages. The first stage is

related with fast processes and propagation of thermal waves before reflection ( $t < \tilde{L}_1 a/v_s$ ). The second stage, related to reflection of thermal wave, begins at  $t = \tilde{L}_1 a/v_s$  and has duration  $t = \tilde{L}_2 a/v_s$ . Finally, the third stage begins after reflection of the wave from boundary at  $t = (\tilde{L}_1 + \tilde{L}_2) a/v_s$  and is related to relaxation of the temperature on the boundary. Evolution of this is presented in figure 4.

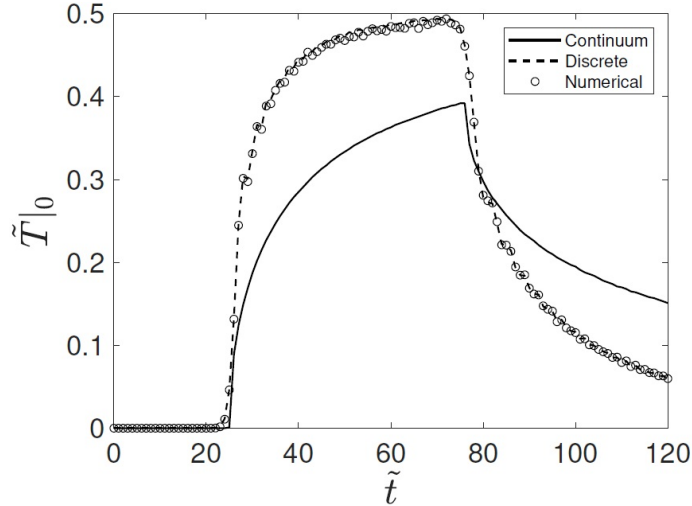


Figure 4: Evolution of the kinetic temperature at the boundary.

One can see from the figure 4, the discrete solution of the kinetic temperature at the boundary significantly differs from the continuum after reaching of thermal wave of the end. Growth of the discrete solution at the boundary, caused by reflection of thermal wave and decrease of this, caused by propagation of wavefront backwards are faster than the same stages of evolution of the continuum solution. Further we show distinguishes of asymptotic behavior of the discrete and continuum solution for the kinetic temperature at the boundary.

Thus, process of heat propagation in the semi-infinite Hooke chain caused by rectangular perturbation can be generally qualitatively described by the continuum model, if we deal with propagation of the wavefront. However, continuum description the field of kinetic temperature at and near the boundary is inapplicable.

### 6.3 Step initial perturbation

We consider step heat perturbation:

$$\tilde{T}^0(\tilde{x}) = H(\tilde{L} - \tilde{x}), \quad \tilde{L} > 0, \quad (35)$$

where  $\tilde{L}a$  is a width of perturbation. Id est, the initial heat pulse affects the boundary. The discrete and continuum kinetic temperatures, corresponding to the case, are presented in figure 5, at  $\tilde{L} = 50$ .

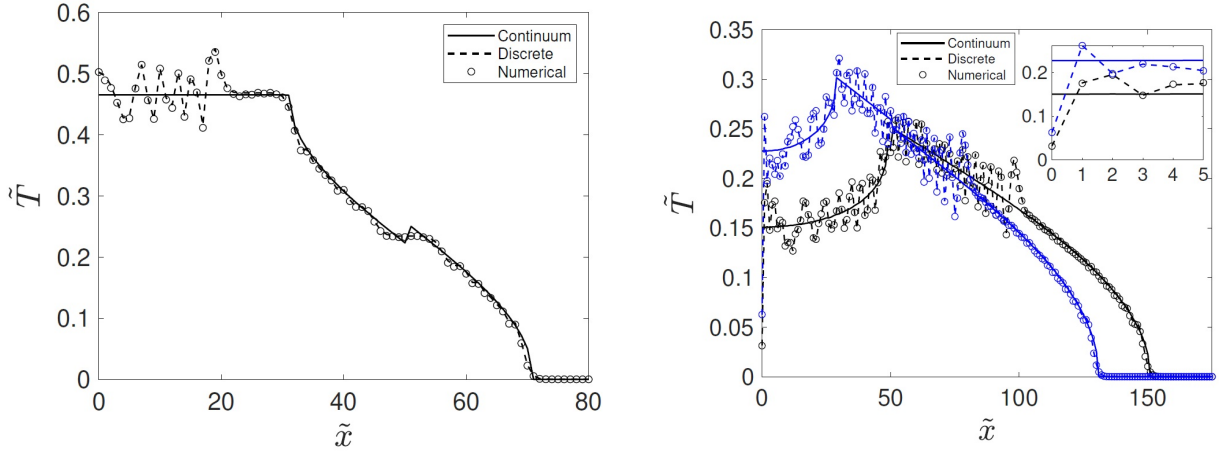


Figure 5: Discrete and continuum kinetic temperatures in the semi-infinite chain corresponding to the cases before ( $\tilde{t} = 20$ , left) and after reflection ( $\tilde{t} = 80$  (blue line) and  $\tilde{t} = 100$  (black line), right).

It is shown in Fig.5 that discrete and continuum solutions are significantly different near the boundary after reflection of thermal wave by virtue of the jump (see inset in right Fig.5). However, some mismatches between discrete and continuum solutions are observed both before ( $t < \tilde{L}a/v_s$ ) and after ( $t > \tilde{L}a/v_s$ ) reflection of thermal wave from the boundary. Before the reflection, these mismatches are caused by influences of the fast process, occurring at the same time of wavefront propagation. The fast process strongly affects on the oscillations of discrete kinetic temperature near the boundary, which cannot be described via the continuum solution. Unexpectedly, mismatches between discrete and continuum kinetic temperature field remain, namely discrete solution diverges from the continuum. The explanation of this divergence is out of frameworks of the present paper. Nevertheless, propagation of the wavefront obeys the continuum solution.

Analogously to 6.2 formula for the continuum kinetic temperature is expressed as:

$$\tilde{T}(0, \tilde{t}) = \frac{H(\tilde{L} - \tilde{t}) + J_0(4\tilde{t})}{2} + \frac{\arcsin\left(\frac{\tilde{L}}{\tilde{t}}\right)}{\pi} H(\tilde{t} - \tilde{L}). \quad (36)$$

Evolution of the kinetic temperature occurs in two stages: equilibration of the kinetic temperature (at times  $\tilde{t} < \tilde{L}$ ). At times ( $\tilde{t} > \tilde{L}$ ) the wavefront propagates after reflection of this from boundary. Then the kinetic temperature on the boundary decays. Changing in time of functions of the temperatures on the boundary are presented in figure 6.

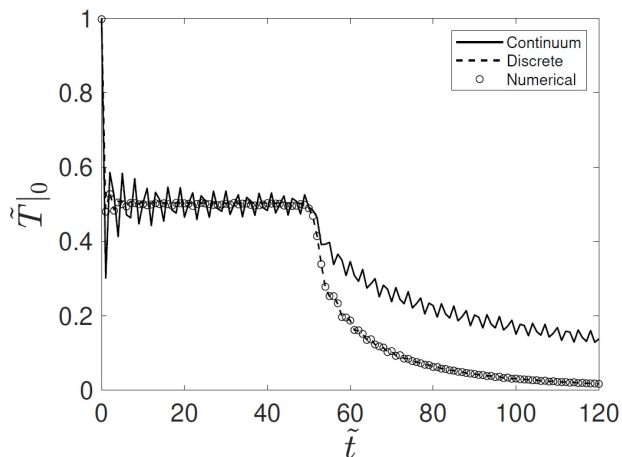


Figure 6: Evolution of the temperature at the boundary.

Figure 6 shows significantly different behavior of the discrete and continuum kinetic temperatures at the large times. Discrete solution decays faster than continuum. According to the preliminary calculations, both discrete and continuum solutions for the kinetic temperature at the boundary are scale invariant with respect to  $\tilde{L}$ . In the next section, we explain how much the discrete solution at the boundary decays faster than continuum.

## 7 Large time asymptotics for the kinetic temperature at the boundary

In the Sect.6 we have revealed that discrete and continuum solutions for the kinetic temperature at the boundary evolve significantly differently at large times. We compare asymptotic behavior for the both solutions in both cases of rectangular and step initial perturbations.

In the case of rectangular perturbation, evolution of the continuum kinetic temperature  $\tilde{T}(0, \tilde{t})$  after reflection of thermal wave obeys the law

$$\tilde{T}(0, \tilde{t}) \simeq \frac{\tilde{L}_2}{\pi \tilde{t}} + O\left(\frac{1}{\tilde{t}^3}\right). \quad (37)$$

In the case of step perturbation, evolution of the continuum kinetic temperature  $\tilde{T}(0, \tilde{t})$  after reflection of thermal wave obeys the law

$$\tilde{T}(0, \tilde{t}) \simeq \sqrt{\frac{1}{2\pi\tilde{t}}} \cos\left(4\tilde{t} - \frac{\pi}{4}\right) + \frac{\tilde{L}}{\pi\tilde{t}} + O\left(\frac{1}{\tilde{t}}\right). \quad (38)$$

Note that asymptotics of (37) does not include asymptotics of the Bessel function. The reason of that is the kinetic temperature at the boundary in case of rectangular perturbation does not undergo oscillations, caused the fast process.

For investigation of the asymptotics of the discrete solution,  $\tilde{T}_0$ , we expand the product of cosines in formula (31). That and substituting  $n = 0$  yields

$$\begin{aligned} \tilde{T}_n &= \sum_{j=0}^{\infty} \tilde{T}_j^0 \left( \sum_{i=1}^4 I_j^i \right)^2, \\ I_j^{1,2} &= \frac{1}{4\pi} \int_{-\pi}^{\pi} \cos\left(\pm j\theta + 2\tilde{t} \sin\frac{\theta}{2}\right) d\theta = \operatorname{Re} \left( \frac{1}{4\pi} \int_{-\pi}^{\pi} e^{i(\pm j\theta + 2\tilde{t} \sin\frac{\theta}{2})} d\theta \right), \\ I_j^{3,4} &= \frac{1}{4\pi} \int_{-\pi}^{\pi} \cos\left(\pm(j+1)\theta + 2\tilde{t} \sin\frac{\theta}{2}\right) d\theta = \operatorname{Re} \left( \frac{1}{4\pi} \int_{-\pi}^{\pi} e^{i(\pm(j+1)\theta + 2\tilde{t} \sin\frac{\theta}{2})} d\theta \right), \quad i^2 = -1. \end{aligned} \quad (39)$$

According to the stationary phase method [26], the main contributions to the integrals  $I_j^i$  have the following form

$$I_j^{1,2} \simeq \pm(-1)^j \sqrt{\frac{1}{4\pi\tilde{t}}} \cos\left(2\tilde{t} - \frac{\pi}{4}\right), \quad I_j^{3,4} \simeq \mp(-1)^j \sqrt{\frac{1}{4\pi\tilde{t}}} \cos\left(2\tilde{t} - \frac{\pi}{4}\right). \quad (40)$$

From (40) it follows that that main contribution (and therefore every contribution) to the integral in (31) equals zero. Therefore, the stationary phase method becomes inapplicable for asymptotic calculation of  $\tilde{T}_0$ .

In order to investigate behavior of the kinetic temperature  $\tilde{T}_0$ , we test function  $\tilde{T}_0 \tilde{t}^\gamma$ , varying the power  $\gamma \in (1; 4)$ . The analysis reveals that for  $\gamma \approx 3$  the discrete kinetic temperature performs non-decaying oscillations for substantially long time (see. Fig.7).

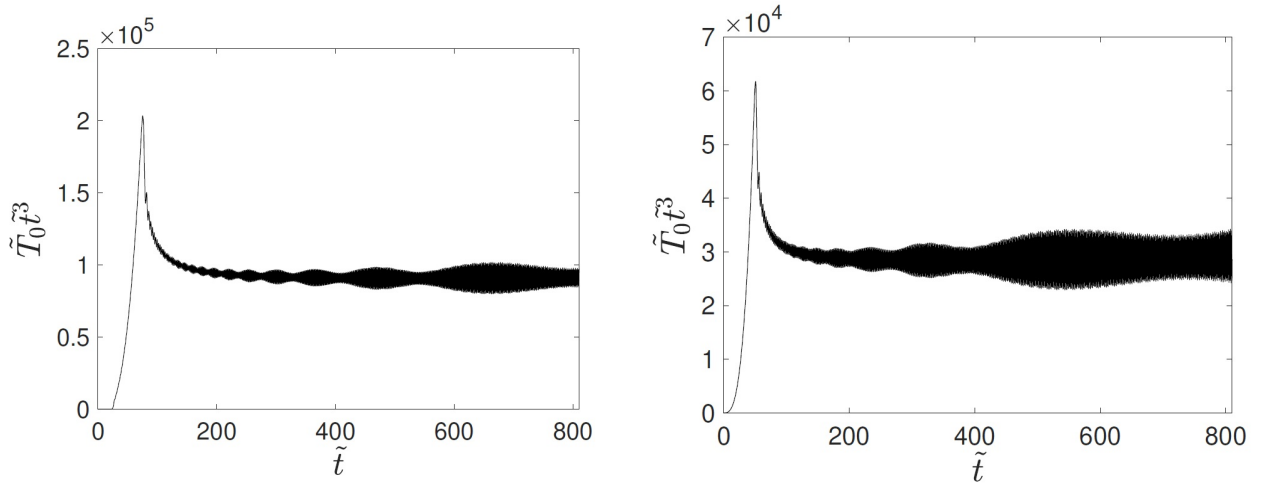


Figure 7: Evolution of the discrete kinetic temperature at the boundary, multiplied by  $\tilde{t}^3$ . Both cases of rectangular (left) and step (right) initial perturbations are under consideration.

Thus, the discrete kinetic temperature at the boundary decays significantly faster than continuum, approximately as  $1/\tilde{t}^3$ . This is one of reasons of that mismatches of continuum and discrete solutions at and near the boundary proceed for a long time. Derivation of the exact asymptotic law for the discrete solution would be an interesting extension of the present work.

## 8 Principle of discrete solution symmetry

In the section, we investigate heat transport in the infinite Hooke chain in the case of initial perturbation determined as

$$\tilde{T}^0(\tilde{x}) = H(\tilde{x} - \tilde{L}_1) - H(\tilde{x} - (\tilde{L}_1 + \tilde{L}_2)) + H(\tilde{x} + (\tilde{L}_1 + \tilde{L}_2)) - H(\tilde{x} + \tilde{L}_1), \quad (41)$$

where the parameters  $\tilde{L}_1$  and  $\tilde{L}_2$  are defined in Sect.6.2. The initial temperature profile (41) assumes two mirrored with respect to zero heat sources.

Further, we consider two cases. The first case is with symmetry of heat sources but the different corresponding initial velocities. Therefore, the governing dynamics equations are

$$\frac{d^2 \tilde{u}_n}{d\tilde{t}^2} = \tilde{u}_{n+1} - 2\tilde{u}_n + \tilde{u}_{n-1}, \quad n = -N, \dots, -2, -1, 0, 1, 2, \dots, N. \quad (42)$$

with initial conditions

$$\tilde{u}_n = 0, \quad \tilde{v}_n = \frac{d\tilde{u}_n}{d\tilde{t}} = \rho_n \sqrt{\tilde{T}_n^0}, \quad \langle \rho_n \rangle = 0, \quad \langle \rho_m \rho_n \rangle = \delta_{mn}, \quad (43)$$

where  $\tilde{T}_n^0$  is determined by the formula (33). Numerically, equations (42–43) are solved with periodic boundary conditions in the same way as discussed in Sect.6.1. In the thermodynamic limit ( $N \rightarrow \infty$ ), analytical solution of the problem is also presented both in the discrete and continuum formulations. The discrete solution for the kinetic temperature is proposed in pioneering work by Klein and Prigogine [15] based on the Schroedinger approach [16] to solving the dynamics equations (42):

$$\tilde{T}_n = \sum_{j=-\infty}^{\infty} \tilde{T}_j^0 J_{2(n-j)}^2(2\tilde{t}). \quad (44)$$

The continuum solution is proposed by Krivtsov [24, 18]:

$$\tilde{T}(\tilde{x}, \tilde{t}) = \frac{\tilde{T}^0(\tilde{x})}{2} J_0(4\tilde{t}) + \frac{1}{2\pi} \int_0^\pi \tilde{T}^0(\tilde{x} + \tilde{t} \cos \theta) d\theta. \quad (45)$$

The discrete and continuum kinetic temperatures for different moments of time and at  $\tilde{L}_1 = 25$ ,  $\tilde{L}_2 = 50$  are presented in Fig. 8.

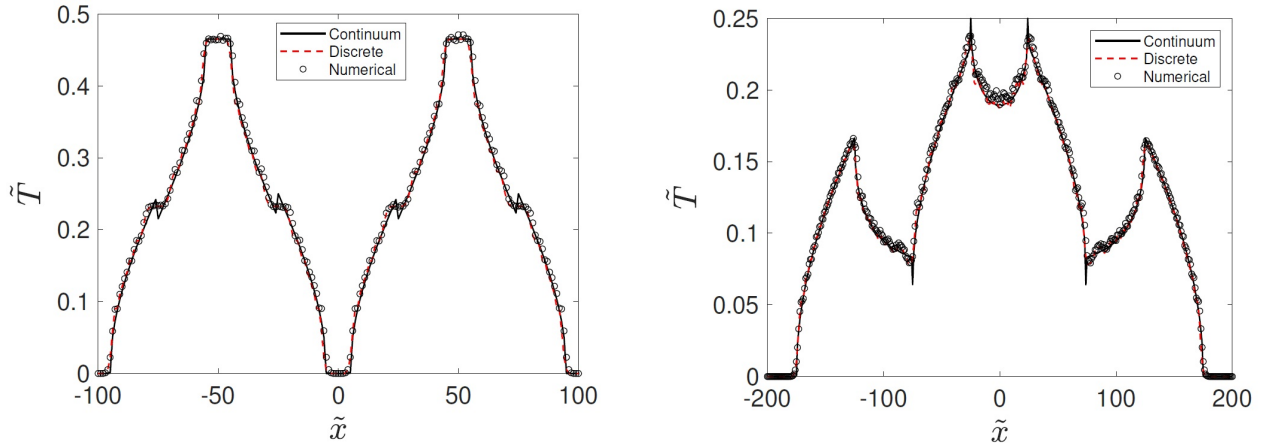


Figure 8: Discrete and continuum solutions for kinetic temperature in the infinite Hooke chain, in the case of rectangular initial perturbation (formula (41)).  $\tilde{t} = 20$  (left) and  $\tilde{t} = 100$  (right).

It is seen from Fig.8 that the continuum and discrete kinetic temperatures are in good agreement. Moreover, in the domain  $\tilde{x} \geq 0$  the continuum kinetic temperature field coincides with the same field in the semi-infinite chain<sup>6</sup>. As expected, the principle of continuum solution principle, formulated in Sect.5 is fulfilled. However, the corresponding discrete solutions disagree. The reason of the mismatch is the random initial velocities are uncorrelated. If so, then the discrete solutions are not symmetric with respect to zero even in case of mirrored heat sources.

Let us consider another case, which is governed by the dynamics equations (28) with initial conditions (29). However, firstly, we enumerate particles as follows:

$$n = -N, \dots, -2, -1, 1, 2, \dots, N. \quad (46)$$

Secondly, we require the following condition for the initial velocities

$$\rho_{-n} = \rho_n, \quad (47)$$

which assumes a symmetry with respect to zero of both initial temperature profile and field of initial velocities simultaneously.

The expression for particle displacement,  $\tilde{u}_n$ , can be represented as

$$\tilde{u}_n = \frac{1}{N} \sum_{k=-N}^{-1} \hat{u}_k e^{i\frac{2\pi kn}{N}} + \frac{1}{N} \sum_{k=1}^N \hat{u}_k^* e^{-i\frac{2\pi kn}{N}}, \quad (48)$$

where  $\hat{u}_k(\tilde{t})$  and  $\hat{u}_k^*(\tilde{t})$  are unknown depending on time functions. From (48), the following representation for  $\tilde{u}_{-n}$  follows

$$\tilde{u}_{-n} = \frac{1}{N} \sum_{k=-N}^{-1} \hat{u}_k e^{-i\frac{2\pi kn}{N}} + \frac{1}{N} \sum_{k=1}^N \hat{u}_k^* e^{i\frac{2\pi kn}{N}}. \quad (49)$$

<sup>6</sup>One can see that, before reflection from the boundary, the discrete kinetic temperature can be described by the solution (44).

The condition (47) must result in  $\hat{u}_k(\tilde{t}) = \hat{u}_k^*(\tilde{t})$ . Therefore,  $\tilde{u}_n = \tilde{u}_{-n}$ . It follows from here that the bond deformation between the particles  $n = -1$  and  $n = 1$  equals zero. Returning to the limit case ( $N \rightarrow \infty$ ), we conclude that the Hooke chain with symmetric with respect to zero field of initial velocities is equivalent to the interacting two semi-infinite free end Hooke chains.

To the best of our knowledge, analytical solution for the kinetic temperature (both in the discrete and continuum formulations), corresponding to the problem (42), (43), (47) is unknown. We calculate numerically the kinetic temperature in the same way as discussed in Sect.6.1 and using periodic boundary conditions <sup>7</sup>. Comparison between kinetic temperature field in the considered model at  $\tilde{t} = 100$  with the corresponding solution for the semi-infinite chain (formulas (32) and (31)) is presented in Fig.9.

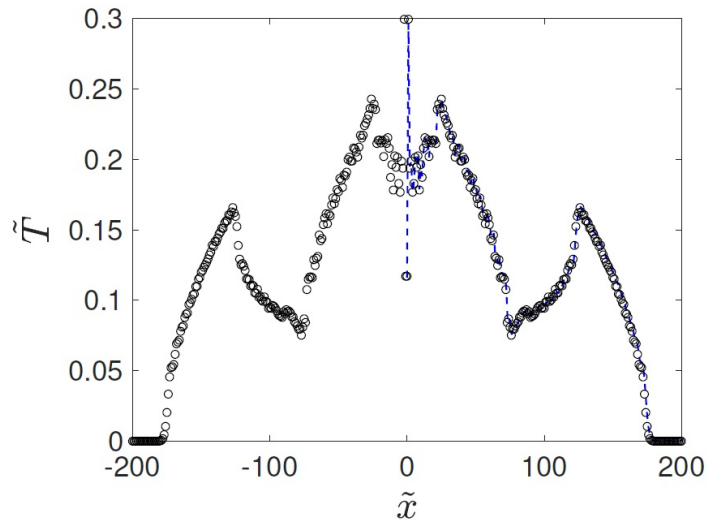


Figure 9: The discrete kinetic temperature profile in the infinite Hooke chain in the case of rectangular initial perturbation (41) with condition (47) (black circles). The discrete kinetic temperature in the semi-infinite free end Hooke chain in the case of rectangular initial perturbation (33) (blue dashed line).

From Fig.9 it is seen that the discrete solution for the semi-infinite chain in case of the rectangular perturbation is the same as solution for the infinite Hooke chain with absolutely mirrored heat sources (with symmetric initial velocity fields with respect to zero).

Thus, the discrete kinetic temperature in the semi-infinite Hooke chain with free end and some field of initial velocities *coincides* with the discrete kinetic temperature in the infinite Hooke chain with the same and mirrored velocity fields. The aforesaid rule will be further referred to as a *principle of discrete solution symmetry*.

## 9 Conclusions

Based on obtained in the paper results, we formulate the following principles, which the mechanism of ballistic heat transport in the semi-infinite free end Hooke chain is satisfied:

1. The continuum kinetic temperature field in the semi-infinite free end Hooke chain with some heat source (initial temperature field) *coincides* with the continuum kinetic temperature

---

<sup>7</sup>In numerical calculations, we enumerate the particles in the sequence (see (42)).

field in the infinite Hooke chain with the same and mirrored with respect to zero heat sources, corresponding to uncorrelated initial velocities. Herewith, the discrete solutions *can mismatch* by virtue of jump of the kinetic temperature near the boundary of the semi-infinite chain. This is the principle of continuum solution symmetry.

2. The discrete kinetic temperature field in the semi-infinite free end Hooke chain with some field of initial velocities *coincides* with the discrete kinetic temperature field in the infinite Hooke chain with the same and mirrored with respect to zero fields of initial velocities. This is the principle of discrete solution symmetry.

The principles may serve to solve the problem of unsteady heat transport problem in the semi-infinite (not only one-dimensional) lattices using known solutions for the infinite lattices.

It was analytically shown that process of ballistic heat propagation in the chain has at least two transient processes. The first is associated with reflection of thermal wave from the free boundary. The second transient process is related with propagation of thermal waves in the same direction. The discrete and continuum solutions for kinetic temperature at the boundary after reflection of thermal wave have significantly different asymptotic behaviors. It is shown heruistically that the exact solution for the kinetic temperature at the boundary decays approximately as  $1/\tilde{t}^3$ .

It was shown by the examples of rectangular and step initial perturbations that the far field of the kinetic temperature obeys the continuum solution (22). However, the discrete and continuum kinetic temperature fields near the boundary mismatch. The continuum description of the ballistic heat transport has restrictions, attributable to the finitenesses. Therefore, the Boltzmann kinetic theory needs taking into account the discreteness of structure. In order to use the continuum solution for kinetic temperature as the constitutive relation, clarification of this with taking into account features of the discrete solution is needed. That can be done in two ways. The first is a stitching of the continuum solution with discrete solution near the boundary. The second way is to solve heat transport problem in infinite chain with mirrored with respect to zero fields of initial velocities and then perform a continualization procedure, proposed in [14] or in [22].

An explanation of jump of the kinetic temperature from free boundary cannot be provided by the model of the semi-infinite chain. In order to understand this, we numerically investigate heat transport through the boundary of the two chains with significantly different stiffnesses. In this system, the jump of the kinetic temperature is the Kapitza jump, which was discovered experimentally long time ago [29]. From these observations, one can assume that the jump of the kinetic temperature near the free end is the limiting case of the Kapitza jump in the two interacting chains with stiffnesses, ratio of which is infinitesimal. However, verifying of this supposition needs a confirmation based on analytical treatments and the problem considered and solved in the present paper, can be auxiliary. Generally speaking, a problem of unsteady heat transport in the heterogeneous lattices is as yet hard to solve analytically but some progress in studying it is attained in the steady-state formulation [30, 31].

## 10 Acknowledgements

The work is supported by the Russian Science Foundation (Grant No. 21-71-10129). The author is deeply grateful to V.A. Kuzkin, A.M. Krivtsov, S.N. Gavrilov, A.S. Sokolov and E.F. Grekova for useful and simulating discussions.

## A Derivation of expression for particle velocities

In order to obtain velocity for any particle, we solve exactly the equation (1) with initial conditions (2). That can be done in two ways. The first is to seek a solution in a form of Bessel function series, proposed in [32], [33]. But this way is cumbersome for further analyzing of the problem. It is optimal to use the eigenfunction expansion method (see [34]). We seek  $u_n$  is the form, satisfying free boundary conditions:

$$u_n = \frac{2}{N} \sum_{k=0}^{N-1} \hat{u}_k \cos \frac{(2n+1)\pi k}{N}, \quad (50)$$

where  $\hat{u}_k$  is a some time-dependent function. Therefore, the direct transform for  $u_n$  to  $\hat{u}_k$  is

$$\hat{u}_k = \sum_{n=0}^{N-1} u_n \cos \frac{(2n+1)\pi k}{N}. \quad (51)$$

Applying (51) to (1) and (2) results in ODE with respect to  $\hat{u}_k$ :

$$\ddot{\hat{u}}_k + \omega_k^2 \hat{u}_k = 0, \quad \omega_k = 2\omega_e \sin \frac{\pi k}{N}, \quad \hat{u}_k|_{t=0} = 0, \quad \dot{\hat{u}}_k|_{t=0} = \sum_{n=0}^{N-1} v_n^0 \cos \frac{(2n+1)\pi k}{N}, \quad (52)$$

whence

$$\hat{u}_k = \frac{\sin(\omega_k t)}{\omega_k} \sum_{n=0}^{N-1} v_n^0 \cos \frac{(2n+1)\pi k}{N}. \quad (53)$$

Substitution of (53) to (50) with subsequent differentiation with respect to time gives the formula (3).

## B Derivation of the discrete fundamental solution

Here, we derive a discrete fundamental solution, namely  $g_{n,j_s}^S(\Delta N)$ .

Expanding a product of cosines in (9) yields

$$\begin{aligned} S_{nj} = & \frac{1}{16\pi^2} \iint_{-\pi}^{\pi} \left[ \cos((n+j+1)(\theta_1 + \theta_2)) + \cos((n+j+1)(\theta_1 - \theta_2)) + \right. \\ & \cos((n-j)(\theta_1 + \theta_2)) + \cos((n-j)(\theta_1 - \theta_2)) + \cos\left(\frac{(2j+1)(\theta_1 + \theta_2)}{2} - \frac{(2n+1)(\theta_1 - \theta_2)}{2}\right) + \\ & \cos\left(\frac{(2j+1)(\theta_1 + \theta_2)}{2} + \frac{(2n+1)(\theta_1 - \theta_2)}{2}\right) + \cos\left(\frac{(2n+1)(\theta_1 + \theta_2)}{2} - \frac{(2j+1)(\theta_1 - \theta_2)}{2}\right) + \\ & \left. \cos\left(\frac{(2n+1)(\theta_1 + \theta_2)}{2} + \frac{(2j+1)(\theta_1 - \theta_2)}{2}\right) \right] \cos((\omega(\theta_1) - \omega(\theta_2))t) d\theta_1 d\theta_2. \end{aligned} \quad (54)$$

Therefore, the expression for  $g_{n,j_s}^S(\Delta N)$  can be rewritten as a sum of the following eight terms:

$$\begin{aligned}
g_{n,j_s}^S(\Delta N) &= \frac{1}{16\pi^2 a} \iint_{-\pi}^{\pi} \cos((\omega(\theta_1) - \omega(\theta_2))t) \sum_{i=1}^8 \varphi_i(\theta_1, \theta_2) d\theta_1 d\theta_2, \\
\varphi_1(\theta_1, \theta_2) &= \frac{1}{2\Delta N} \sum_{j=j_s-\Delta N+1}^{j_s+\Delta N} \cos((n+j+1)(\theta_1+\theta_2)) = \\
&= \frac{1}{2\Delta N} \cos\left(\frac{3(\theta_1+\theta_2)}{2} + (\theta_1+\theta_2)(n+j_s)\right) \frac{\sin((\theta_1+\theta_2)\Delta N)}{\sin\left(\frac{\theta_1+\theta_2}{2}\right)}, \\
\varphi_2(\theta_1, \theta_2) &= \frac{1}{2\Delta N} \sum_{j=j_s-\Delta N+1}^{j_s+\Delta N} \cos((n+j+1)\Delta\theta) = \frac{1}{2\Delta N} \cos\left(\left(n+j_s+\frac{3}{2}\right)\Delta\theta\right) \frac{\sin(\Delta N\Delta\theta)}{\sin\frac{\Delta\theta}{2}}, \\
\varphi_3(\theta_1, \theta_2) &= \frac{1}{2\Delta N} \sum_{j=j_s-\Delta N+1}^{j_s+\Delta N} \cos((n-j)(\theta_1+\theta_2)) = \frac{1}{2\Delta N} \cos\left((\theta_1+\theta_2)\left(\frac{1}{2}+j_s-n\right)\right) \\
&= \frac{\sin((\theta_1+\theta_2)\Delta N)}{\sin\left(\frac{\theta_1+\theta_2}{2}\right)}, \\
\varphi_4(\theta_1, \theta_2) &= \frac{1}{2\Delta N} \sum_{j=j_s-\Delta N+1}^{j_s+\Delta N} \cos((n-j)\Delta\theta) = \frac{1}{2\Delta N} \cos\left(\Delta\theta\left(\frac{1}{2}+j_s-n\right)\right) \frac{\sin(\Delta N\Delta\theta)}{\sin\frac{\Delta\theta}{2}}, \\
& \tag{55} \\
\varphi_5(\theta_1, \theta_2) &= \frac{1}{2\Delta N} \sum_{j=j_s-\Delta N+1}^{j_s+\Delta N} \cos\left(\frac{(2j+1)(\theta_1+\theta_2)}{2} - \frac{(2n+1)(\theta_1-\theta_2)}{2}\right) = \\
&= \frac{1}{2\Delta N} \cos\left(\theta_1\left(\frac{1}{2}+j_s-n\right) + \theta_2\left(\frac{3}{2}+j_s+n\right)\right) \frac{\sin((\theta_1+\theta_2)\Delta N)}{\sin\left(\frac{\theta_1+\theta_2}{2}\right)}, \\
\varphi_6(\theta_1, \theta_2) &= \frac{1}{2\Delta N} \sum_{j=j_s-\Delta N+1}^{j_s+\Delta N} \cos\left(\frac{(2j+1)(\theta_1+\theta_2)}{2} + \frac{(2n+1)(\theta_1-\theta_2)}{2}\right) = \\
&= \frac{1}{2\Delta N} \cos\left(\theta_2\left(\frac{1}{2}+j_s-n\right) + \theta_1\left(\frac{3}{2}+j_s+n\right)\right) \frac{\sin((\theta_1+\theta_2)\Delta N)}{\sin\left(\frac{\theta_1+\theta_2}{2}\right)}, \\
\varphi_7(\theta_1, \theta_2) &= \frac{1}{2\Delta N} \sum_{j=j_s-\Delta N+1}^{j_s+\Delta N} \cos\left(\frac{(2n+1)(\theta_1+\theta_2)}{2} - \frac{(2j+1)(\theta_1-\theta_2)}{2}\right) = \\
&= \frac{1}{2\Delta N} \cos\left(\theta_1\left(\frac{1}{2}+j_s-n\right) - \theta_2\left(\frac{3}{2}+j_s+n\right)\right) \frac{\sin(\Delta N\Delta\theta)}{\sin\left(\frac{\Delta\theta}{2}\right)}, \\
\varphi_8(\theta_1, \theta_2) &= \frac{1}{2\Delta N} \sum_{j=j_s-\Delta N+1}^{j_s+\Delta N} \cos\left(\frac{(2n+1)(\theta_1+\theta_2)}{2} + \frac{(2j+1)(\theta_1-\theta_2)}{2}\right) = \\
&= \frac{1}{2\Delta N} \cos\left(\theta_2\left(\frac{1}{2}+j_s-n\right) - \theta_1\left(\frac{3}{2}+j_s+n\right)\right) \frac{\sin(\Delta N\Delta\theta)}{\sin\left(\frac{\Delta\theta}{2}\right)}, \quad \Delta\theta = \theta_1 - \theta_2.
\end{aligned}$$

We rewrite the components  $\varphi_2, \varphi_4, \varphi_7, \varphi_8$ , containing the difference of wave numbers  $\Delta\theta$  as

follows:

$$\begin{aligned}
\varphi_2 &= \frac{\Delta\theta}{2} \left[ \frac{\cos \frac{3\Delta\theta}{2}}{\sin \frac{\Delta\theta}{2}} (\cos((n+j_s)\Delta\theta)) - \frac{\sin \frac{3\Delta\theta}{2}}{\sin \frac{\Delta\theta}{2}} (\sin((n+j_s)\Delta\theta)) \right] \text{sinc}(\Delta N \Delta\theta), \\
\text{sinc}(x) &= \frac{\sin x}{x}, \\
\varphi_4 &= \frac{\Delta\theta}{2} \left[ \cot \frac{\Delta\theta}{2} \cos((n-j_s)\Delta\theta) + \sin((n-j_s)\Delta\theta) \right] \text{sinc}(\Delta N \Delta\theta), \\
\varphi_7 &= \frac{\Delta\theta}{2} \left[ \frac{\cos \frac{3\Delta\theta}{2}}{\sin \frac{\Delta\theta}{2}} \cos(\Delta\theta(n+j_s) - \theta_1(2n+1)) - \frac{\sin \frac{3\Delta\theta}{2}}{\sin \frac{\Delta\theta}{2}} \sin(\Delta\theta(n+j_s) - \theta_1(2n+1)) \right] \\
&\text{sinc}(\Delta N \Delta\theta), \\
\varphi_8 &= \frac{\Delta\theta}{2} \left[ \cot \frac{\Delta\theta}{2} \cos(\theta_1(2n+1) - \Delta\theta(n-j_s)) - \sin(\theta_1(2n+1) - \Delta\theta(n-j_s)) \right] \\
&\text{sinc}(\Delta N \Delta\theta).
\end{aligned} \tag{56}$$

The formula (56) can be simplified due to our assumptions about continualization. At  $\Delta N \gg 1$ , the function  $\text{sinc}(x)$  is equal to 1 if  $\Delta\theta$  is zero and fast tends to zero if  $\Delta\theta$  is not equal to zero. Therefore, the main contribution, to the function  $g_{n,j_s}^S(\Delta N)$  comes from two close wavenumbers  $\theta_1, \theta_2$ . Therefore, in the limit cases of  $\Delta\theta \rightarrow 0$  and  $\Delta N \gg 1$ , we have

$$\begin{aligned}
\varphi_2 &= \cos((n+j_s)\Delta\theta) \text{sinc}(\Delta N \Delta\theta) + O\left(\frac{1}{\Delta N}\right), \\
\varphi_4 &= \cos((n-j_s)\Delta\theta) \text{sinc}(\Delta N \Delta\theta) + O\left(\frac{1}{\Delta N}\right), \\
\varphi_7 &= \cos(\theta_1(2n+1) - (n+j_s)\Delta\theta) \text{sinc}(\Delta N \Delta\theta) + O\left(\frac{1}{\Delta N}\right), \\
\varphi_8 &= \cos(\theta_1(2n+1) - (n-j_s)\Delta\theta) \text{sinc}(\Delta N \Delta\theta) + O\left(\frac{1}{\Delta N}\right), \\
\varphi_1 &= \varphi_3 = \varphi_5 = \varphi_6 = O\left(\frac{1}{\Delta N}\right).
\end{aligned} \tag{57}$$

The difference  $\omega(\theta_1) - \omega(\theta_2)$  can be decomposed into series:

$$\omega(\theta_1) - \omega(\theta_2) \approx \omega'(\theta_1) \Delta\theta. \tag{58}$$

Substitution of (57), (58) to (55) with dropping out of the terms of order  $O\left(\frac{1}{\Delta N}\right)$  gives the formula (11).

## C Derivation of formulas for wave-packets in the limit of mesoscale

We show that approximation of expressions for wave packets in (12) in the limit case ( $\Delta N \gg 1$ ) approaches us to the Fourier transform of the sinc function.

Indeed,

$$\begin{aligned}
\frac{1}{2\pi a} \int_{\theta-\pi}^{\theta+\pi} \cos(q\Xi) \text{sinc}(q\Delta N) dq &= \frac{1}{2\pi a \Delta N} \int_{(\theta-\pi)\Delta N}^{(\theta+\pi)\Delta N} \cos\left(\frac{q\Xi}{\Delta N}\right) \text{sinc} q dq \\
&\approx \frac{1}{2\pi a \Delta N} \int_{-\infty}^{\infty} \cos\left(\frac{q\Xi}{\Delta N}\right) \text{sinc} q dq = \text{Re} \left( \frac{1}{2\pi a \Delta N} \int_{-\infty}^{\infty} e^{i\left(\frac{q\Xi}{\Delta N}\right)} \text{sinc} q dq \right).
\end{aligned} \tag{59}$$

Analogously,

$$\frac{1}{2\pi a} \int_{\theta-\pi}^{\theta+\pi} \sin(q\Xi) \text{sinc}(q\Delta N) dq \approx \text{Im} \left( \frac{1}{2\pi a \Delta N} \int_{-\infty}^{\infty} e^{i\left(\frac{q\Xi}{\Delta N}\right)} \text{sinc} q dq \right). \quad (60)$$

Since (see e.g. [35])

$$\frac{1}{2\pi} \int_{-\infty}^{\infty} e^{i\xi q} \text{sinc} q dq = \frac{1}{2} H(1 - |\xi|), \quad (61)$$

then one gets

$$\begin{aligned} \frac{1}{2\pi a \Delta N} \int_{-\infty}^{\infty} \cos\left(\frac{q\Xi}{\Delta N}\right) \text{sinc} q dq &= \frac{1}{2a \Delta N} H\left(1 - \frac{|\Xi|}{\Delta N}\right), \\ \frac{1}{2\pi a \Delta N} \int_{-\infty}^{\infty} \sin\left(\frac{q\Xi}{\Delta N}\right) \text{sinc} q dq &= 0. \end{aligned} \quad (62)$$

## References

- [1] Rickert, W., Vilchevskaya, E.N., Müller, W.H. A note on Couette flow of micropolar fluids according to Eringen's theory Vol. 7, No. 1, 25–50 (2019)
- [2] Lepri, S., Livi, R., Politi, A.: Thermal conduction in classical low-dimensional lattices. Phys. Rep. 377, 1 (2003)
- [3] Dhar A., Heat transport in low-dimensional systems. Advances in Physics, pp. 457-537, (2008)
- [4] Chang, C.W. Thermal transport in low dimensions. In: Lecture Notes in Physics, vol. 921, pp. 305–338 (2016)
- [5] Huberman, S., Duncan, R.A., Chen, K., Song, B., Chiloyan, V., Ding, Z., Maznev, A.A., Chen, G., Nelson, K.A.: Observation of second sound in graphite at temperatures above 100 K. Science (2019)
- [6] Johnson, J.A., Maznev, A.A., Cuffe, J., Eliason, J.K., Minnich, A.J., Kehoe, T., Sotomayor, Torres, C.M., Chen, G., Nelson, K.A.: Direct measurement of room-temperature nondiffusive thermal transport over micron distances in a silicon membrane. Phys. Rev. Lett. 110, 025901 (2013)
- [7] Anufriev, R., Gluchko, S. Volz, S. Nomura, M. Quasi-ballistic heat conduction due to Levy phonon flights in silicon nanowires. Mesoscale and Nanoscale Physics (2018)
- [8] Chang, C.W., Okawa, D., Garcia, H., Majumdar, A., Zettl, A.: Breakdown of Fourier's law in nanotube thermal conductors. Phys. Rev. Lett. 101, 075903 (2008)
- [9] Xu, X., Wang Yu, Zhang, K et al. Length-dependent thermal conductivity in suspended single-layer graphene. Nature Communications (2014)
- [10] Dwivedi, N., Ott, A.K., Sasikumar K., Dou, C., Yeo, R.J., Narayanan, B., et c. Graphene Overcoats for Ultra-High Storage Density Magnetic Media (2019)
- [11] Majumdar, A. Microscale Heat Conduction in Dielectric Thin Films, J. Heat Transfer, 115(1): 7-16 (1993)

- [12] Cahill, D.G., Ford, W.K., Goodson, K.E., Mahan, G.D., Majumdar, A., Maris, H.J., Merlin, R., Phillpot, S.R.: Nanoscale thermal transport. *J. Appl. Phys.* 93, 793 (2003)
- [13] Spohn, H.: The phonon Boltzmann equation, properties and link to weakly anharmonic lattice dynamics. *J. Stat. Phys.* 124(2–4), 1041–1104 (2006)
- [14] Kuzkin, V.A., Krivtsov, A.M. Unsteady ballistic heat transport: linking lattice dynamics and kinetic theory. *ActaMechanica* (2021)
- [15] Klein, G., Prigogine, I. Sur la mecanique statistique des phenomenes irreversibles III. *Physica*, Vol. 19, 1053 (1953)
- [16] Schrödinger, E. Zur dynamik elastisch gekoppelter punktsysteme. *Annalen der Physik*, Vol. 44, p. 916, (1914)
- [17] Sokolov, A.A., Müller, W.H., Porubov, A.V., Gavrilov, S.N. Heat conduction in 1D harmonic crystal: Discrete and continuum approaches. *International Journal of Heat and Mass Transfer*, Vol. 176, 121442 (2021)
- [18] Krivtsov, A.M. Heat transfer in infinite harmonic one dimensional crystals. *Dokl. Phys.* 60(9), 407 (2015)
- [19] Sokolov, A.A., Krivtsov, A.M., Muller, W.H.: Localized heat perturbation in harmonic 1D crystals: solutions for an equation of anomalous heat conduction. *Phys. Mesomech.* 20(3), 305–310 (2017)
- [20] Northrop G.A. and Wolfe J.P. Phonon Imaging: Theory and Applications. *Nonequilibrium Phonon Dynamics* pp. 165-242 (1985)
- [21] Wolfe, James P.. Imaging phonons. *Acoustic wave propagation in solids*. Cambridge University Press (1998)
- [22] Gavrilov, S.N., Krivtsov, A.M., Tsvetkov, D.V.: Heat transfer in a one-dimensional harmonic crystal in a viscous environment subjected to an external heat supply. *Cont. Mech. Thermodyn.* 31(1), 255–272 (2019)
- [23] Kuzkin, V.A. Unsteady ballistic heat transport in harmonic crystals with polyatomic unit cell. *Continuum Mechanics and Thermodynamics*, 26 p. (2019)
- [24] Krivtsov, A.,M. Energy Oscillations in a One-Dimensional Crystal. *Doklady Physics.* 2014, Vol. 59, No. 9, pp. 427–430
- [25] Gelfand, I., Shilov, G.: *Generalized Functions. Properties and Operations*, vol. 1. Academic Press, New York (1964)
- [26] Fedoryuk, M.V.: The stationary phase method and pseudodifferential operators. *Russ.Math. Surv.* 6(1), 65–115 (1971) (in Russian)
- [27] Candy, J and Rozmus, W. A symplectic integration algorithm for separable Hamiltonian functions, *J. Comput. Phys.* 92, 230 (1991)
- [28] McLachlan, R.I. and Atela, P. The accuracy of symplectic integrators, *Nonlinearity* 5, 541 (1992)
- [29] Kapitza, P.L. The Study of Heat Transfer in Helium II, *J. Phys. USSR* 4, 181 (1941)

- [30] Gendelman, O.V. and Paul, J. Kapitza thermal resistance in linear and nonlinear chain models: Isotopic Defect, Phys. Rev. E 103, 052113 (2021)
- [31] Gendelman, O.V. and Paul, J. Kapitza resistance at a domain boundary in linear and nonlinear chains, Phys. Rev. E 104, 054119 (2021)
- [32] Hemmer, P.C. Dynamic and stochastic types of motion in the linear chain. Norges tekniske hoiskole, (1959)
- [33] Takizawa, E, Kobayasi, K. On the Stochastic Types of Motion in a System of Linear Harmonic Oscillators. Chinese Journal of Physics, Vol. 6, No.1 (1967)
- [34] Mandel'shtam, L.I. Polnoe Sobranie Trudov (Complete Collected Works) (Ed. S M Rytov) Vol. 1 (Moscow: Izd. AN SSSR, 1948) (in Russian)
- [35] Ango, A. Mathematics for Electro- and Radio Engineers. Nauka, Moscow (1965).